

# Coherence Transfer Signals in the Rotational Resonance NMR of a Spinning Single Crystal

Oleg N. Antzutkin\*<sup>1</sup> and Malcolm H. Levitt†

\*Division of Inorganic Chemistry, Luleå University of Technology, S-971 87 Luleå, Sweden; and †Physical Chemistry Division, Arrhenius Laboratory, Stockholm University, S-10691 Stockholm, Sweden

Received March 14, 2000; revised July 19, 2000

**A recent analysis of rotational resonance lineshapes (M. Helmle *et al.*, *J. Magn. Reson.* **140**, 379–403, 1999) predicted the existence of coherence transfer signals, which are generated by mechanically induced coherence transfer during the detection process. These signals correspond to the generation of observable coherences at spin sites that have no magnetization at the beginning of the observation interval but which acquire coherence while the detection is underway. The coherence transfer signals disappear for powder samples in conventional magic-angle-spinning solid-state NMR experiments. In this Communication, we report the successful detection of coherence transfer signals in rotor-synchronized experiments performed on a single crystal of [1,2-<sup>13</sup>C<sub>2</sub>]glycine. © 2000 Academic Press**

**Key Words:** CP/MAS <sup>13</sup>C NMR; single crystal; rotational resonance; coherence transfer signals.

Rotational resonance experiments (1–9) are now routinely used for internuclear accurate distance measurements in a wide range of biologically relevant systems which cannot be crystallized for X-ray diffraction studies and which are inaccessible to liquid-state NMR. Examples include biomembranes (10, 11), amyloid (12, 13) and prion (14) peptides, protein–drug complexes (15), and membrane proteins (16, 17). For isolated homonuclear spin-1/2 pairs, spin transitions are driven mechanically by adjusting the spinning frequency  $\omega_r$  to match the rotational resonance condition,  $\omega_{\Delta}^{\text{iso}} = n_{\text{RR}}\omega_r$ , where  $\omega_{\Delta}^{\text{iso}}$  is the isotropic shift frequency difference and  $n_{\text{RR}}$  is a small integer. At this condition, one observes spectral broadenings or splittings which are proportional to the through-space dipole–dipole coupling between the spins (4, 5). The dipole couplings may also be estimated by measuring the exchange of Zeeman magnetization between the sites (4, 5). The dipole–dipole coupling constant,  $b_{ij}$ , is a simple function of the interspin distance,  $r_{ij}$ :  $b_{ij} = -(\mu_0/8\pi^2)(\gamma^2 h/r_{ij}^3)$ , and may be used to estimate both intra- and intermolecular distances.

Recently, an extended theory of rotational resonance spectra was developed (9). This theory predicted two main effects: (i) the nontrivial influence of transverse relaxation on the rotational resonance lineshapes, in the case that the involved spins have dif-

ferent coherence decay rate constants, and (ii) the existence of coherence transfer signals at rotational resonance, caused by mechanically driven coherence transfer during the signal acquisition. The first prediction of the extended theory (the nontrivial relaxation effects) has been well-tested by experiment (9). The second prediction (the coherence transfer signals) has never been experimentally verified, to our knowledge. These signals correspond to the generation of observable coherences at spin sites that are not directly excited by the radiofrequency pulse sequence. The signals may also be predicted using the original theory of rotational resonance spectra, but were overlooked in the original papers on the subject (1–5). In this Communication we present a first experimental observation of rotational resonance coherence transfer signals for a single crystal of [<sup>13</sup>C<sub>2</sub>]glycine mounted in the magic-angle-spinning rotor.

Consider a solid containing isolated homonuclear spin pairs of spins-1/2 in sites  $j$  and  $k$ . Suppose that the spin density operator at the beginning of the detection period (defined as  $t = 0$ ) is given by  $\rho(0) \sim -S_{jy}$ , which implies that only  $j$  sites are initially magnetized. This initial state may be prepared by either selective cross-polarization or frequency-selective excitation of the spins in sites  $j$ . The NMR signal at rotational resonance consists of four components: two “direct” signals  $s_a^{j \rightarrow j}$  and  $s_b^{j \rightarrow j}$ , and two coherence transfer signals  $s_a^{j \rightarrow k}$  and  $s_b^{j \rightarrow k}$ . The expressions for these signals are given by Eqs. [74]–[81] of Ref. (9), which are reproduced here:

$$s_a^{j \rightarrow j}(t) = \frac{1}{2} \exp\{i(\omega_j^{\text{iso}} + \pi J_{jk})t - \bar{r}t\} \times \left[ \cosh\left(\frac{1}{2} Rt\right) - \frac{r_{\Delta}}{R} \sinh\left(\frac{1}{2} Rt\right) \right] \quad [1a]$$

$$s_b^{j \rightarrow j}(t) = \frac{1}{2} \exp\{i(\omega_j^{\text{iso}} - \pi J_{jk})t - \bar{r}t\} \times \left[ \cosh\left(\frac{1}{2} Rt\right) - \frac{r_{\Delta}}{R} \sinh\left(\frac{1}{2} Rt\right) \right] \quad [1b]$$

<sup>1</sup>To whom correspondence should be addressed. Fax: +46-920-91199. E-mail: Oleg.Antzutkin@km.luth.se.

$$s_a^{j \rightarrow k}(t) = \frac{i\omega_B^{(n)*}}{2R} \exp\{i(\omega_k^{\text{iso}} + \pi J_{jk})t - \bar{r}t\} \sinh\left(\frac{1}{2}Rt\right) \quad [1c]$$

$$s_b^{j \rightarrow k}(t) = -\frac{i\omega_B^{(n)*}}{2R} \exp\{i(\omega_k^{\text{iso}} - \pi J_{jk})t - \bar{r}t\} \sinh\left(\frac{1}{2}Rt\right). \quad [1d]$$

Here  $\omega_j^{\text{iso}}$  and  $\omega_k^{\text{iso}}$  are isotropic chemical shift frequencies of sites  $j$  and  $k$ , respectively.  $J_{jk}$  is the isotropic  $J$ -coupling,  $\bar{r} = (r_j + r_k)/2$ ,  $r_\Delta = (r_j - r_k)$ , and  $R^2 = r_\Delta^2 - |\omega_B^{(n)}|^2$  with  $r_j$  and  $r_k$  equal to the transverse relaxation rate constants of the sites, and  $\omega_B^{(n)}$  is the resonant Fourier component of the homonuclear spin–spin coupling, defined by Eqs. [12]–[14] in Ref. (9). Although these equations take into account the lineshape anomalies caused by differential transverse relaxation, it should be emphasized that the coherence transfer signals  $s_a^{j \rightarrow k}$  and  $s_b^{j \rightarrow k}$  also appear when relaxation is not taken into account. The direct signals are generated by coherences that are excited at the beginning of the detection period, while the coherence transfer signals contain frequencies close to the precession frequency of spins  $k$  which are *not* magnetized at the beginning of signal acquisition. The latter signals are generated by mechanically induced transfer of coherence from sites  $j$  to sites  $k$  during the detection period. The two indirect signals,  $s_a^{j \rightarrow k}$  and  $s_b^{j \rightarrow k}$ , have frequencies which differ by the  $J$ -coupling and have opposite amplitudes. As a result, these signals cancel out if the  $J$ -coupling is unresolved. In addition, the phase of the coherence transfer signals depends strongly on the molecular orientation angle  $\gamma_{\text{MR}}$  and the initial sample rotation angle  $\alpha_{\text{RL}}^0$  according to Eq. [82] of Ref. (9):

$$\arg\{\omega_B^{(n)}(\alpha_{\text{MR}}, \beta_{\text{MR}}, \gamma_{\text{MR}})^*\} = n(\gamma_{\text{MR}} + \alpha_{\text{RL}}^0). \quad [2]$$

Here, the standard notion for Euler angles is used (5):  $\Omega_{\text{MR}} = \{\alpha_{\text{MR}}, \beta_{\text{MR}}, \gamma_{\text{MR}}\}$  characterizes the orientation of the molecular reference frame  $\text{M}$  with respect to the rotor reference frame  $\text{R}$ , and  $\Omega_{\text{RL}} = \{\alpha_{\text{RL}}^0 - \omega_r t, \beta_{\text{RL}} = \text{Arccos}(1/\sqrt{3}), 0\}$  describes the relative orientation of  $\text{M}$  and the laboratory reference frame  $\text{L}$ , which is fixed with respect to the external magnetic field. The angle  $\alpha_{\text{RL}}^0$  defines the initial rotor position at time  $t = 0$  (defined as the start of signal acquisition) and is under experimental control by synchronizing the radiofrequency pulse sequence with the optical tachometer signal (18, 19). Equation [2] implies that the coherence transfer signals disappear for finely divided powders (averaging over  $\gamma_{\text{MR}}$ ) and for unsynchronized experiments on spinning oriented samples provided that extensive signal averaging is performed (averaging over  $\alpha_{\text{RL}}^0$ ).

The observation of coherence transfer signals therefore requires four conditions to be satisfied: (i) resolved  $J$ -couplings; (ii) selective polarization of one of the coupled spin sites; (iii) incomplete averaging over  $\gamma_{\text{MR}}$ ; (iv) incomplete averaging over

$\alpha_{\text{RL}}^0$ . Condition (i) may be satisfied by a suitable choice of sample and spectrometer conditions; condition (ii) may be satisfied by choosing a suitable initial pulse sequence; condition (iii) may be satisfied by using a spinning sample with orientational order, such as a spinning single crystal. Condition (iv) may be satisfied by synchronizing the pulse sequence with the sample rotation. For the case of a spinning single crystal in a rotor-synchronized experiment, both angles  $\gamma_{\text{MR}}$  and  $\alpha_{\text{RL}}^0$  are fixed, and the coherence transfer signals may be observed, provided that additional crystal symmetries do not cause additional destructive interference. The latter might occur if the crystal space group contains several molecules in the unit cell and if the crystal orientation is unfavorable.

For the experimental demonstration of the coherence transfer signals, a single crystal of [ $^{13}\text{C}_2$ ]glycine, of approximate dimensions  $4 \times 4 \times 3$  mm and mass 23.8 mg, was grown by slow evaporation of an aqueous solution of 99% [ $1,2\text{-}^{13}\text{C}_2$ ]glycine (obtained from Cambridge Isotope Laboratories, Andover, MA, and used without further purification). The crystal was surrounded by Teflon tape and packed into a standard zirconium dioxide double-bearing 6-mm rotor (Chemagnetics). All experiments were performed on a Chemagnetics Infinity CMX-400 ( $B_0 = 9.4$  T) spectrometer using cross-polarization from the protons together with proton decoupling (20). The  $^{13}\text{C}$  Larmor frequency was  $-100.83$  MHz (21, 22). The proton  $\pi/2$  pulse duration was  $4.5 \mu\text{s}$  and the nutation frequencies of protons and carbons during cross-polarization and decoupling were  $\omega_{\text{CP}}(^1\text{H})/2\pi = \omega_{\text{CP}}(^{13}\text{C})/2\pi = 55$  kHz and  $\omega_{\text{dec}}(^1\text{H})/2\pi = 90$  kHz.

The required initial condition for the spin density operator at the beginning of the detection period,  $\rho(0) \sim -S_{j_y}$ , in which only one set of spin sites is initially magnetized, was achieved by selective cross-polarization from the protons (20). In glycine it is possible to create a predominant magnetization of only  $\text{CH}_2$ -carbons by using a short Hartmann–Hahn contact interval. Carboxyl carbons cross-polarize slowly since they do not have directly bonded protons. Aliphatic carbons, on the other hand, are relatively well-magnetized even at short contact intervals of the order of 0.01–0.1 ms. Signals deriving from non-cross-polarized  $^{13}\text{C}$  magnetization are removed by phase cycling of the initial proton  $\pi/2$  pulse.

Figure 1 shows  $^{13}\text{C}$  NMR spectra of the [ $1,2\text{-}^{13}\text{C}_2$ ]glycine crystal at a spinning frequency of  $\omega_r/2\pi = 5720$  Hz, which is approximately midway between the  $n = 2$  and 3 rotational resonance conditions ( $\omega_\Delta^{\text{iso}}/2\pi = 13.440$  kHz). The CP-contact interval was set to 0.02 ms. Under these cross-polarization conditions the signal from aliphatic carbon sites dominates. The carboxyl peak is very weak. The rotor-synchronized (Fig. 1a) and unsynchronized (Fig. 1b) spectra are qualitatively very similar. A splitting of approximately 50 Hz, due to the  $^{15}\text{C}$ – $^{13}\text{C}$   $J$ -coupling, is visible for both carbon peaks in the unsynchronized spectrum shown in Fig. 1b. There are some minor differences of detail between the two spectra, such as the difference of the phases and intensities of the spinning sidebands

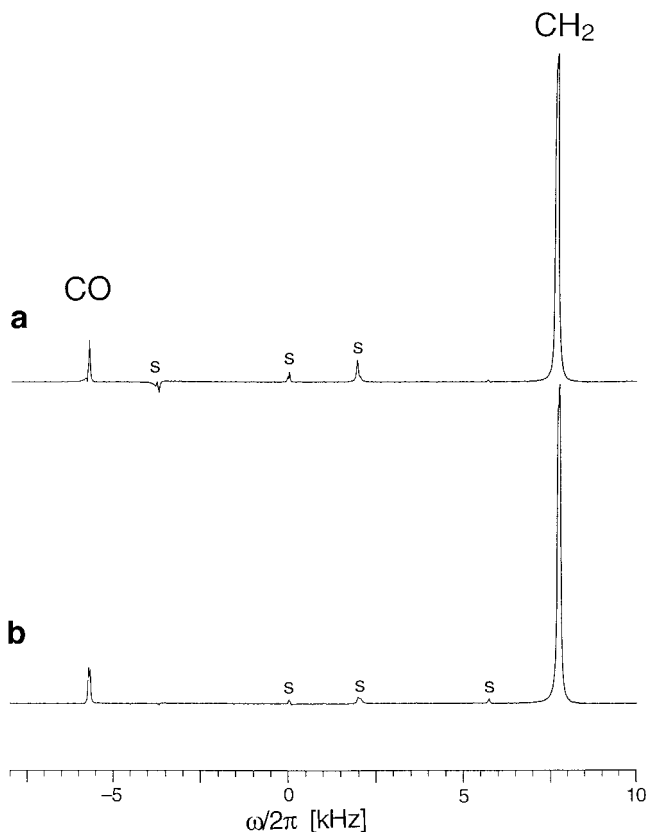


**FIG. 1.**  $^{13}\text{C}$  CP/MAS spectra of a  $[1,2-^{13}\text{C}_2]$ glycine single crystal spun at a rotor frequency  $\omega_r/2\pi = 5720$  Hz which is well off the  $n = 2$  and 3 rotational resonance conditions. A short contact interval of 0.02 ms was used for the selective cross-polarization of methylene carbon sites. (a) Synchronized and (b) unsynchronized CP/MAS spectra. Sixty-four transients were used in both cases. Spinning sidebands are marked with "s."

(which are slightly more intense in the synchronized experiments, as expected for oriented systems (23)) and the absence of one of the doublet components of the CO peak in the synchronized spectrum of Fig. 1a. The latter small discrepancies are not fully understood, but may be due to weak rotor-driven coherence transfer signals in the coupled spin system, giving rise to small peak shape perturbations even far from rotational resonance.

At the  $n = 2$  rotational resonance condition, which was achieved by spinning at  $\omega_r/2\pi = 6720$  Hz, an additional splitting of approximately 400 Hz is observed for the methylene carbon peak. In the rotor-synchronized experiment (Fig. 2a), strong antiphase signals also appear close to the frequency of the carboxyl  $^{13}\text{C}$  site. These are the coherence transfer signals (indicated by "CTS" in Fig. 2a). As predicted, these signals average out when the synchronization is removed and many transients are added together (Fig. 2b).

The shape of the coherence transfer signals qualitatively follows the predicted pattern of peaks with alternating positive and negative amplitudes. Signal  $s_a^{j \rightarrow k}$  is represented in the spectrum by the second left (negative) and fourth (positive)

peaks of the coherence transfer signals (this shape is described by the anti-symmetric  $\sinh(Rt/2)$  function in Eq. [1c]), while the other two lines of the coherence transfer signals are given by  $s_b^{j \rightarrow k}$  in Eq. [1d].  $s_a^{j \rightarrow k}$  and  $s_b^{j \rightarrow k}$  have opposite sign and are shifted with respect to each other by  $J_{jk} \approx 50$  Hz as is readily seen in Fig. 2a.

The coherence transfer signals in Fig. 2a are approximately as intense as the "conventional" NMR signals on the right-hand side of the spectra in Fig. 2. Remarkably, the appearance of the large coherence transfer signals does not deplete the amplitude of the conventional signals. In some circumstances it may be possible to exploit these additional signals to enhance the sensitivity of NMR spectra acquired at rotational resonance. In the limit, it may be possible to recover the loss in signal strength associated with the splitting of the NMR peaks at rotational resonance.

The phase of the coherence transfer signals given in Eq. [2] depends on the synchronization angle  $\alpha_{\text{RL}}^0$ , which defines the rotor position at the time point  $t = 0$ , according to  $n\alpha_{\text{RL}}^0$  where  $n$  is the order of rotational resonance. It is possible to choose

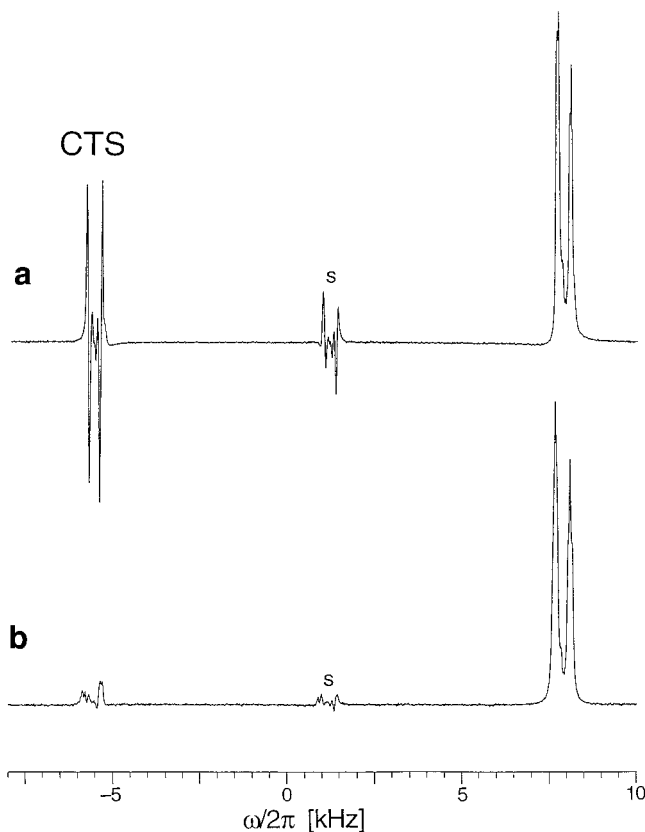


**FIG. 2.** As in Fig. 1 but with a spinning frequency satisfying the  $n = 2$  rotational resonance condition ( $\omega_r/2\pi = 6720$  Hz). (a) Rotor-synchronized spectrum. Strong coherence transfer signals are detected as the carboxyl carbon sites (indicated by "CTS"). (b) Unsynchronized spectrum. The coherence transfer signals are canceled by signal averaging over the synchronization angle  $\alpha_{\text{RL}}^0$ . Sixty-four transients were used in both cases. "s" Denotes spinning sidebands.

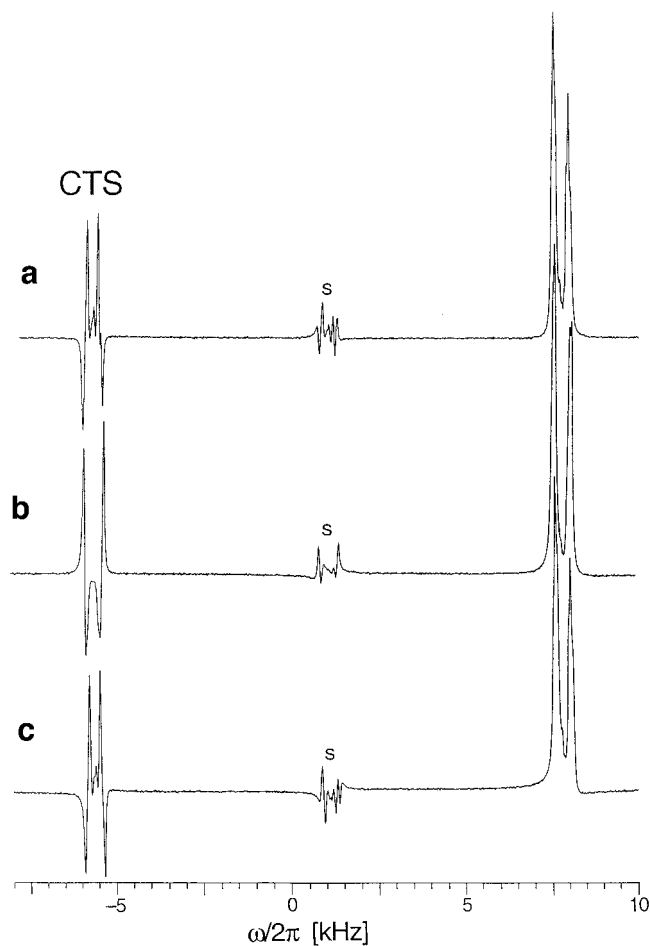


**FIG. 3.**  $^{13}\text{C}$  CP/MAS rotor-synchronized spectra of a  $[1,2-^{13}\text{C}_2]$ glycine single crystal using different synchronization delays. The delays correspond to the following values of  $\alpha_{\text{RL}}^0$  (relative to the spectrum shown in Fig. 2a): (a)  $270^\circ$ , (b)  $180^\circ$ , and (c)  $90^\circ$ . The same phase correction was applied to all spectra, including those in Figs. 1 and 2. Note the strong dependence of the phase of the coherence transfer signals on the synchronization angle  $\alpha_{\text{RL}}^0$ .

an arbitrary value for the synchronization angle  $\alpha_{\text{RL}}^0$  by changing the delay between the synchronization time point at the start of the pulse sequence. Figure 3 shows rotor-synchronized spectra of the  $[1,2-^{13}\text{C}_2]$ glycine crystal with different values of  $\alpha_{\text{RL}}^0$  (relative to that used in Fig. 2a):  $270^\circ$  (Fig. 3a);  $180^\circ$  (Fig. 3b), and  $90^\circ$  (Fig. 3c). The phases of the coherence transfer signals depend on  $2\alpha_{\text{RL}}^0$ , as expected for the  $n = 2$  rotational resonance. Note that the direct  $\text{CH}_2$  signals are almost independent of the synchronization angle  $\alpha_{\text{RL}}^0$  (see Figs. 2 and 3) as predicted by Eqs. [1a] and [1b]. The slight phase dependence of the  $\text{CH}_2$  signals on  $\alpha_{\text{RL}}^0$  is probably due to chemical shift anisotropy.

We have also obtained rotor-synchronized spectra of the  $[1,2-^{13}\text{C}_2]$ glycine crystal at the  $n = 3$  and 4 rotational resonance conditions. These signals also showed coherence transfer signals at frequencies close to the carboxyl  $^{13}\text{C}$  precession

frequency (spectra not shown). The properties of these signals were also in agreement with Eqs. [1] and [2].

In conclusion, we have demonstrated experimentally the existence of coherence transfer signals, by recording rotor-synchronized spectra of a  $[1,2-^{13}\text{C}_2]$ glycine single crystal at rotational resonance. These signals are caused by mechanically induced coherence transfer between two sets of spins during the signal detection period. The mechanical coherence transfer process leads to the appearance of NMR signal in spectral regions which were not directly excited by the pulse sequence. The amplitudes, frequencies, and phases of the coherence transfer signals are in qualitative agreement with the predictions of Ref. (9).

The coherence transfer signals in rotational resonance NMR are related to the phenomenon of coherent Raman beats (CRB), observed in optical and microwave spectroscopy (24–28), as well as in ordinary NMR (29). In the CRB phenomenon, the existence of a coherence between two closely spaced energy eigenstates is revealed as the modulation of the transition amplitude between one of these levels and a distant level. It is possible to use this effect to detect nuclear or electronic sub-level coherences indirectly through modulations of the optical and microwave emission (24–28). In the rotational resonance case, the two  $M = 0$  states of the four-level system represent the “closely spaced” levels, while a  $M = \pm 1$  state represents the distant level. The radiofrequency signal associated with the coherence between a  $M = 0$  state and one of the  $M = \pm 1$  states is modulated by the rotor-driven oscillations between the two  $M = 0$  states.

As mentioned above, the coherence transfer signals might be useful in some circumstances for enhancing the sensitivity of rotational resonance NMR. In addition, these signals could allow one to obtain molecular angular information from ordered biomolecular samples (30–32). As demonstrated in Fig. 3, the phases of the coherence transfer signals are highly sensitive to one of the molecular orientational angles. In principle, such spectra could be used to orient the directions of  $^{13}\text{C}$ – $^{13}\text{C}$  vectors with respect to an external order axis. It may also be possible to detect rotational resonance coherence transfer signals in powders by using orientation-dependent excitation techniques (33).

## ACKNOWLEDGMENTS

We thank Dr. R. Tycko for instrument time and Dr. Y. Ishii for advice on growing a large single crystal of glycine. M. H. L. was supported by the Swedish Natural Science Research Council and by the Göran Gustafsson Foundation for Research in the Natural Sciences and Medicine.

## REFERENCES

1. E. R. Andrew, A. Bradbury, R. G. Eades, and V. T. Wynn, *Phys. Lett.* **4**, 99 (1963).
2. E. R. Andrew, S. Clough, L. F. Farnell, T. D. Gledhill, and I. Roberts, *Phys. Lett.* **21**, 505 (1966).

3. M. G. Colombo, B. H. Meier, and R. R. Ernst, *Chem. Phys. Lett.* **146**, 189 (1988).
4. D. P. Raleigh, M. H. Levitt, and R. G. Griffin, *Chem. Phys. Lett.* **146**, 71 (1988).
5. M. H. Levitt, D. P. Raleigh, F. Creuzet, and R. G. Griffin, *J. Chem. Phys.* **92**, 6347 (1990).
6. T. Karlsson, M. Helmle, N. D. Kurur, and M. H. Levitt, *Chem. Phys. Lett.* **247**, 534 (1995).
7. T. Karlsson and M. H. Levitt, *J. Chem. Phys.* **109**, 5493 (1998).
8. X. Feng, P. J. E. Verdegem, Y. K. Lee, M. Helmle, S. C. Shekar, J. Lugtenburg, H. J. M. de Groot, and M. H. Levitt, *Solid State NMR* **14**, 81 (1999).
9. M. Helmle, Y. K. Lee, P. J. E. Verdegem, X. Feng, T. Karlsson, J. Lugtenburg, H. J. M. de Groot, and M. H. Levitt, *J. Magn. Reson.* **140**, 379 (1999).
10. O. B. Peersen, S. Yoshimura, H. Hojo, S. Aimoto, and S. O. Smith, *J. Am. Chem. Soc.* **114**, 4332 (1992).
11. S. O. Smith, *Curr. Opin. Struct. Biol.* **3**, 755 (1993).
12. P. T. Lansbury, P. R. Costa, J. M. Griffiths, E. J. Simon, M. Auger, K. J. Halverson, D. A. Kocisko, Z. S. Hendsch, T. T. Ashburn, R. G. S. Spencer, P. Tidor, and R. G. Griffin, *Nat. Struct. Biol.* **2**, 990 (1995).
13. P. R. Costa, D. A. Kocisko, B. Q. Sun, P. T. Lansbury, and R. G. Griffin, *J. Am. Chem. Soc.* **119**, 10487 (1997).
14. J. Heller, A. C. Kolbert, R. Larsen, M. Ernst, T. Bekker, M. Baldwin, S. B. Prusiner, A. Pines, and D. Wemmer, *Protein Sci.* **5**, 1655 (1996).
15. D. A. Middleton, R. Robins, X. Feng, M. H. Levitt, I. D. Spiers, C. H. Schwalbe, D. G. Reid, and A. Watts, *FEBS Lett.* **410**, 269 (1997).
16. F. Creuzet, A. McDermott, R. Gebhardt, K. van der Hoef, M. B. Spijker-Assink, J. Herzfeld, J. Lugtenburg, M. H. Levitt, and R. G. Griffin, *Science* **251**, 783 (1991).
17. P. J. E. Verdegem, M. Helmle, J. Lugtenburg, and H. J. M. de Groot, *J. Am. Chem. Soc.* **119**, 169 (1997).
18. G. S. Harbison, V.-D. Vogt, and H. W. Spiess, *J. Chem. Phys.* **86**, 1206 (1987).
19. A. Hagemeyer, K. Schmidt-Rohr, and H. W. Spiess, *Adv. Magn. Reson.* **13**, 85 (1989).
20. A. Pines, M. G. Gibby, and J. S. Waugh, *J. Chem. Phys.* **56**, 1776 (1972).
21. M. H. Levitt, *J. Magn. Reson.* **126**, 164 (1997).
22. M. H. Levitt and O. G. Johannessen, *J. Magn. Reson.* **142**, 190 (2000).
23. O. N. Antzutkin and M. H. Levitt, *J. Magn. Reson. A* **118**, 295 (1996).
24. R. L. Shoemaker and R. G. Brewer, *Phys. Rev. Lett.* **28**, 1430 (1972).
25. R. G. Brewer and E. L. Hahn, *Phys. Rev. A* **11**, 1641 (1975).
26. M. K. Bowman, R. J. Massoth, and C. S. Yannoni, in "Pulsed Magnetic Resonance: NMR, ESR and Optics" (D. M. S. Bagguley, Ed.), p. 42, Clarendon Press, Oxford, 1992.
27. T. Blasberg and D. Suter, *Phys. Rev. B* **51**, 6309 (1995).
28. E. L. Hahn, *J. Magn. Reson. A* **116**, 230 (1995).
29. C. S. Yannoni, R. D. Kendrick, and P. G. Wang, *Phys. Rev. Lett.* **58**, 345 (1987).
30. Z. Song, O. N. Antzutkin, A. Rupprecht, and M. H. Levitt, *Chem. Phys. Lett.* **253**, 349 (1996).
31. Z. Song, O. N. Antzutkin, Y. K. Lee, S. C. Shekar, A. Rupprecht, and M. H. Levitt, *Biophys. J.* **73**, 1539 (1997).
32. C. Glaubitz and A. Watts, *J. Magn. Reson.* **130**, 305 (1998).
33. O. N. Antzutkin, *Prog. Nucl. Magn. Reson. Spectrosc.* **35**, 203 (1999).